

## Electronic Supplementary Information

### Development of ultra-high affinity bivalent ligands targeting the polo-like kinase 1

Kohei Tsuji,<sup>a,b</sup> David Hymel,<sup>a,c</sup> Buyong Ma,<sup>d,e</sup> Hirokazu Tamamura,<sup>b</sup> Ruth Nussinov,<sup>d</sup>  
Terrence R. Burke, Jr.<sup>a,\*</sup>

<sup>a</sup>Chemical Biology Laboratory, Center for Cancer Research, National Cancer Institute,  
National Institutes of Health, Frederick, MD 21702, USA

<sup>b</sup>Department of Medicinal Chemistry, Institute of Biomaterials and Bioengineering, Tokyo  
Medical and Dental University, Tokyo 101-0062, Japan

<sup>c</sup>Current affiliation; Discovery Chemistry, Novo Nordisk Research Center Seattle, Seattle,  
WA 98109, USA

<sup>d</sup>Computational Structural Biology Section, Laboratory of Immunometabolism, Frederick  
National Laboratory for Cancer Research, National Cancer Institute at Frederick, Frederick,  
MD 21702, USA

<sup>e</sup>Current affiliation: Engineering Research Center of Cell & Therapeutic Antibody (MOE),  
School of Pharmacy, Shanghai Jiaotong University, Shanghai, 200240, China

\*Correspondence to T. R. Burke, Jr., E-mail: [burkete@mail.nih.gov](mailto:burkete@mail.nih.gov); Fax: 301-846-6033

<b>Contents</b>	<b>Page</b>
<b>I. SYNTHETIC PROCEDURES</b>	
1. General procedures	S5
2. General Fmoc-based solid-phase peptide synthesis (SPPS) protocols for the synthesis of bivalent ligands	S6
3. Synthesis of bivalent ligands <b>3 – 10</b>	S7
4. Synthesis of <b>FITC-2</b>	S8
5. Synthesis of <b>Lys(BI2536*)</b>	S8
6. Synthesis of <b>Lys(BI2536<sup>†</sup>)</b>	S10
7. Synthesis of bivalent ligands <b>11 – 14</b>	S12
8. Synthesis of bivalent ligands <b>15 and 16</b>	S13
9. Synthesis of bivalent ligand <b>17</b>	S14
10. Analytical HPLC data for peptides <b>3 – 17</b> and <b>FITC-2</b>	S16
<b>II. BIOLOGICAL EVALUATION</b>	
1. Expression and purification of full-length Polo-like kinase 1 (Plk1) and isolated Plk1 polo-box domain (PBD) for fluorescence polarization (FP) assays, kinase assays, and fluorescence recovery assays	S19
2. FP assays using purified full-length Plk1	S20
3. Kinase enzymatic assays using purified full-length Plk1	S20
4. Fluorescence recovery assays using purified full-length Plk1	S21
5. MTT assays using HeLa cells	S22
6. Immunostaining experiments using HeLa cells	S22
<b>III. MOLECULAR DYNAMICS SIMULATIONS</b>	<b>S29</b>
<b>IV. CELL MEMBRANE PERMEABILITY ANALYSIS</b>	<b>S31</b>
<b>SCHEMES</b>	

Scheme S1. Synthesis of bivalent ligands <b>3 – 10</b>	S7
Scheme S2. Synthesis of <b>FITC-2</b>	S8
Scheme S3. Synthesis of <b>Lys(BI2536*)</b>	S8
Scheme S4. Synthesis of <b>Lys(BI2536<sup>†</sup>)</b>	S10
Scheme S5. Synthesis of bivalent ligands <b>11 – 14</b>	S12
Scheme S6. Synthesis of bivalent ligands <b>15 – 16</b>	S13
Scheme S7. Synthesis of a bivalent ligand <b>17</b>	S14

## TABLE

Table S1. Characterized data of synthesized peptides	S15
Table S2. Molecular dynamics simulation parameters	S30
Table S3. Results from Caco-2 cell permeability assays of <b>17</b>	S31

## FIGURES

Figure S1. The structure of probe <b>S6</b>	S21
Figure S2. Results from FP assays of initial bivalent ligands <b>3</b> and <b>4</b> against full-length Plk1 and isolated Plk1 PBD	S23
Figure S3. Results from kinase assays of initial bivalent ligands <b>3</b> and <b>4</b> against full-length Plk1	S24
Figure S4. Results from fluorescence recovery assays of initial bivalent ligands <b>3</b> and <b>4</b> and bivalent ligands having attenuated KD binding moieties <b>11 – 14</b> against full-length Plk1	S24
Figure S5. Results from FP assays of bivalent ligands having different length linker <b>3 – 10</b> against full-length Plk1	S25
Figure S6. Results from FP and fluorescence recovery assays of <b>3</b> and <b>9</b> with various concentration of non-labelled probes as competitors against full-length Plk1	S25

Figure S7. Results from FP assays of bivalent ligands having attenuated KD binding moieties <b>11 – 14</b> against full-length Plk1	S26
Figure S8. Results from kinase assays of bivalent ligands having attenuated KD binding moieties <b>11 – 14</b> against full-length Plk1	S26
Figure S9. Results from FP assays of bivalent ligands having attenuated PBD binding moieties <b>15</b> and <b>16</b> against full-length Plk1	S27
Figure S10. Results from FP assays of a bivalent ligand possessing hydrolytically stable pT mimetic Pmab <b>17</b> against full-length Plk1	S27
Figure S11. Results from fluorescence recovery assays of a bivalent ligand possessing hydrolytically stable pT mimetic Pmab <b>17</b> against full-length Plk1	S28
Figure S12. Results from MTT assays of bivalent ligands having no PEG linker <b>9</b> and <b>17</b> against HeLa cells	S28
<b>REFERENCES</b>	S32

## I. SYNTHETIC PROCEDURES

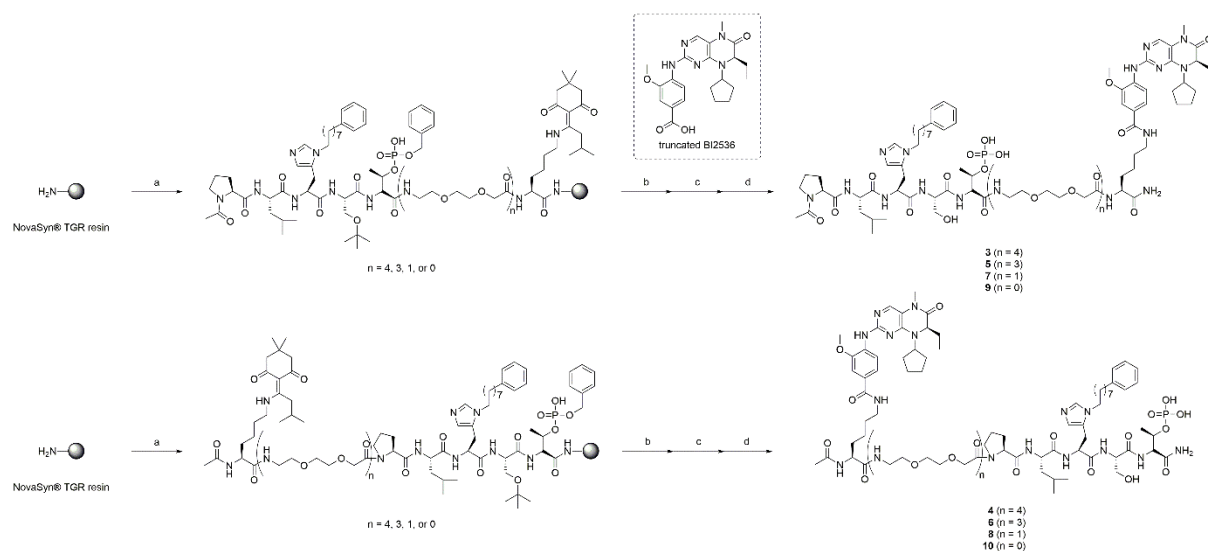
**1. General procedure.** All experiments involving moisture-sensitive compounds were conducted under anhydrous conditions (positive argon pressure) using standard syringe, cannula, and septa apparatus. Commercial reagents were purchased from Sigma, TCI America, Acros, Alfa Aesar, Chem-Impex, or Novabiochem. All solvents were purchased in anhydrous form (Aldrich) and used without further drying. HPLC-grade hexanes, EtOAc, dichloromethane (DCM), and MeOH were used for chromatography. Silica gel column chromatography employed a Teledyne CombiFlash Rf 200 instrument with either EtOAc/hexane or MeOH/DCM gradients. Nuclear Magnetic Resonance (NMR) spectra were recorded using a Varian Inova 400 MHz or 500 MHz spectrometer. Coupling constants are reported in Hertz, and peak shifts are reported in  $\delta$  (ppm) relative to  $\text{CDCl}_3$  ( $^1\text{H}$  7.26 ppm,  $^{13}\text{C}$  77.16 ppm), MeOD ( $^1\text{H}$  3.31 ppm,  $^{13}\text{C}$  49.00 ppm), or dimethyl sulfoxide ( $\text{DMSO}$ )- $d_6$  ( $^1\text{H}$  2.50 ppm,  $^{13}\text{C}$  39.52 ppm). High resolution mass spectra (HRMS) were obtained by positive ion, electrospray ionization (ESI) analysis on a Thermo Scientific LTQ-XL Orbitrap mass spectrometer with high performance liquid chromatography (HPLC) sample introduction using a short narrow-bore  $\text{C}_{18}$  reversed-phase column with MeCN- $\text{H}_2\text{O}$  gradients. Preparative HPLC purification was performed using a Waters 2545 binary pump (0.1% TFA in MeCN/0.1% trifluoroacetic acid (TFA) in  $\text{H}_2\text{O}$  gradient) with a Phenomenex Gemini- $\text{C}_{18}$  (5  $\mu\text{m}$ , 250 x 21 mm) preparative column at a flow rate of  $10 \text{ cm}^3 \text{ min}^{-1}$  with UV detection at 210 nm and a Cosmosil 5 $\text{C}_{18}$ -ARII column (20 x 250 mm, Nacalai Tesque, Inc., Japan) on a JASCO PU-2087 plus (JASCO Corporation, Ltd., Japan) at a flow rate of  $10 \text{ cm}^3 \text{ min}^{-1}$  with UV detection at 210 nm. Semi-preparative HPLC purification was performed using an Agilent 1200 series quaternary pump (0.1% TFA in MeCN/0.1% TFA in  $\text{H}_2\text{O}$  gradient) with a Phenomenex Kinetix- $\text{C}_{18}$  (5  $\mu\text{m}$ , 250 x 10 mm) semi-preparative column, 3 mL/min flow rate with UV detection at 210 nm. Analytical HPLC analyses of purified peptides were performed using an

Agilent 1200 series quaternary pump (0.1% TFA in MeCN/0.1% TFA in H<sub>2</sub>O gradient) with a Phenomenex Gemini-C<sub>18</sub> (5 μm, 250 x 4 mm) analytical column, 1 mL/min flow rate with UV detection at 210 nm and a Cosmosil 5C<sub>18</sub>-ARII column (4.6 × 250 mm, Nacalai Tesque, Inc.) on a PU-2089 plus (JASCO Corporation, Ltd.) at a flow rate of 1.0 cm<sup>3</sup> min<sup>-1</sup>, and eluting products were detected by UV at 210 nm. HPLC eluents were A: 0.1% TFA in H<sub>2</sub>O; B: 0.1% TFA in MeCN.

**2. General Fmoc-based solid-phase peptide synthesis (SPPS) protocols for the synthesis of bivalent ligands.** NovaSyn<sup>®</sup> TGR resin (Novabiochem, 0.25 mmol/g) was pre-swollen in *N*-methylpyrrolidone (NMP) for 20 min with shaking. The following loading procedure was used where applicable. 9-Fluorenylmethyloxycarbonyl (Fmoc)-protected amino acids (2.0 – 4.0 equivalents based on resin loading) were dissolved in NMP and pre-activated by the addition of 1-[bis(dimethylamino)methylene]-1*H*-1,2,3-triazolo[4,5-*b*]pyridinium 3-oxide hexafluorophosphate (HATU, 0.95 mole-equivalents relative to the amino acid) and *N,N*-diisopropylethylamine (DIPEA, 2.0 mole-equivalents relative to the amino acid) with shaking (1 min). The resin was washed with NMP, and the HATU-activated amino acid solution was added to the washed resin. Coupling reactions were shaken at room temperature and allowed to proceed from 2 h to overnight, depending on the equivalents used and the steric bulk of each amino acid. Coupling reactions were routinely checked for completion using a Kaiser test. Once completed, the resin was filtered and washed with NMP, followed by Fmoc-deprotection using 20% piperidine in DMF for 10 min with shaking. Deprotection of the 1-(4,4-dimethyl-2,6-dioxocyclohex-1-ylidene)-3-methylbutyl (ivDde) group on the Lys ε-amine group was performed by treatment with 2% (v/v) hydrazine monohydrate in NMP (two times for 3 h to overnight each). The resin was subsequently coupled with truncated BI2536 (1.0 equivalents based on resin loading) using HATU (0.95 mole-equivalents relative to the amino acid) and

DIPEA (2.0 mole-equivalents relative to the amino acid) at room temperature with shaking (from 3 h to overnight, twice). After completion of the coupling, the complete resins were washed with dichloromethane (DCM) and dried *in vacuo*. Cleavage from the finished resin with global deprotection was achieved using a cocktail of TFA/TIPS/H<sub>2</sub>O = 95:2.5:2.5 (2.0 mL/50 mg resin, 2 h, twice). The mixture was filtered and concentrated under a stream of N<sub>2</sub>. The resulting crude material was dissolved in 0.1% TFA containing MeCN and H<sub>2</sub>O and subjected to preparative reverse-phase HPLC purification. Further purification was conducted using semi-preparative reverse-phase HPLC when needed.

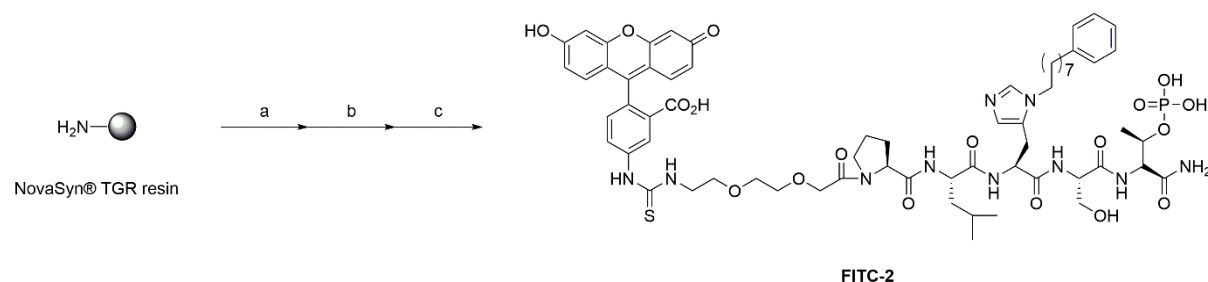
### 3. Synthesis of bivalent ligands 3 – 10.



**Scheme S1.** Synthesis of bivalent ligands **3** – **10**. (a) Fmoc-based SPPS; (b) 2% (v/v) hydrazine monohydrate in NMP; (c) truncated BI2536, HATU, DIPEA, NMP; (d) TFA/TIPS/H<sub>2</sub>O = 95:2.5:2.5.

The synthesis of bivalent ligands **3** – **10** was achieved following the general Fmoc-based SPPS protocols mentioned above. The characterized data of these synthesized peptides are shown in the Table S1.

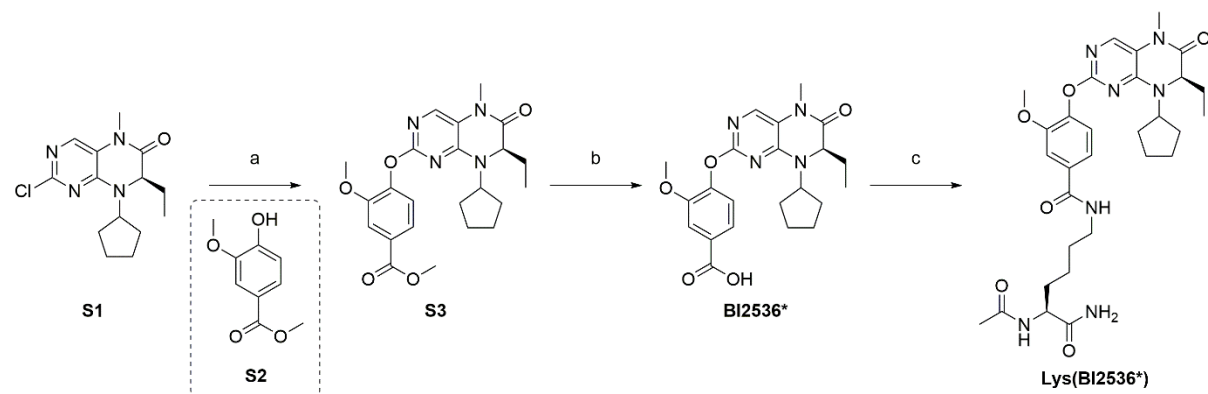
#### 4. Synthesis of FITC-2.



**Scheme S2.** Synthesis of **FITC-2**. (a) Fmoc-based SPPS; (b) FITC, DIPEA, NMP; (c) TFA/TIPS/H<sub>2</sub>O = 95:2.5:2.5.

The synthesis of **FITC-2** was achieved following the general Fmoc-based SPPS protocols mentioned above, and the N-terminal FITC modification was conducted by the treatment of FITC (2.0 equivalents based on resin loading) and DIPEA (4.0 equivalents based on resin loading) in NMP with shaking overnight at room temperature. The characterized data of the synthesized peptide is shown in the Table S1.

#### 5. Synthesis of Lys(BI2536\*).



**Scheme S3.** Synthesis of **Lys(BI2536\*)**. (a) **S2**, Cs<sub>2</sub>CO<sub>3</sub>, DMSO; (b) LiOH, THF/H<sub>2</sub>O = 1:1; (c) Ac-Lys(NH<sub>2</sub>·HCl)-NH<sub>2</sub>, HOBt, EDC·HCl, DMF.

To a solution of (*R*)-2-chloro-8-cyclopentyl-7-ethyl-5-methyl-7,8-dihydropteridin-6(5H)-one (**S1**, 200 mg, 0.68 mmol)<sup>1</sup> and methyl 4-hydroxy-3-methoxybenzoate (**S2**, 150 mg,



0.81 mmol) in DMSO (2.0 mL) was added Cs<sub>2</sub>CO<sub>3</sub> (270 mg, 0.81 mmol). The reaction mixture was stirred at 90 to 95 °C for 4 d. The mixture was roughly purified by preparative HPLC (0 to 95% B in A over 30 min) to yield crude methyl (*R*)-4-((8-cyclopentyl-7-ethyl-5-methyl-6-oxo-5,6,7,8-tetrahydropteridin-2-yl)oxy)-3-methoxybenzoate (**S3**)·2TFA salt (94 mg,.) and the obtained **S3** was used for next step without further purification.

**S3**·2TFA salt (94 mg, 0.14 mmol) and LiOH (17 mg, 0.70 mmol) were dissolved in a solvent mixture of THF (1.0 mL) and H<sub>2</sub>O (1.0 mL). The reaction mixture was stirred at room temperature for 2 d. The mixture was purified by CombiFlash silica gel column chromatography (0 to 35% of MeOH in DCM over 12 min, and then 35 to 100% of MeOH in DCM over 2 min) to yield (*R*)-4-((8-cyclopentyl-7-ethyl-5-methyl-6-oxo-5,6,7,8-tetrahydropteridin-2-yl)oxy)-3-methoxybenzoic acid (**BI2536\***, 57 mg, 20%, 2 steps from **S1**) as white to beige powder.

<sup>1</sup>H NMR (400 MHz, MeOD) δ 7.74 (s, 1H), 7.72–7.69 (m, 2H), 7.22–7.20 (m, 1H), 4.25 (dd, *J* = 6.4 Hz and 3.3 Hz, 1H), 3.79 (s, 3H), 3.61 (quin, *J* = 9.0 Hz, 1H), 3.33 (s, 3H), 1.98–1.87 (m, 2H), 1.84–1.73 (m, 2H), 1.67–1.55 (m, 2H), 1.32–1.19 (m, 3H), 1.17–1.09 (m, 1H), 0.78 (t, *J* = 7.5 Hz, 3H).

<sup>13</sup>C NMR (101 MHz, MeOD) δ 165.6, 161.3, 153.9, 153.0, 147.6, 138.9, 124.1, 123.7, 119.7, 114.5, 64.8, 63.6, 56.3, 29.0, 28.6, 28.4, 28.0, 24.6, 24.4, 8.6.

HRMS (ESI+) calculated for C<sub>22</sub>H<sub>27</sub>N<sub>4</sub>O<sub>5</sub>: 427.1976 [M+H]<sup>+</sup>; found: 427.1962.

To a solution of **BI2536\*** (15 mg, 0.035 mmol) in DMF (1.0 mL) was added HOBt (5.2 mg, 0.039 mmol) followed by addition of 1-ethyl-3-(3-dimethylaminopropyl)carbodiimide·HCl (EDC·HCl, 6.7 mg, 0.035 mmol) and stirring at room temperature for 10 min. In the another flask, to a solution of Ac-Lys(NH<sub>2</sub>·HCl)-NH<sub>2</sub> (8.7 mg, 0.039 mmol) in DMF (0.5 mL) was added DIPEA (13 μL, 0.077 mmol) and the mixture was

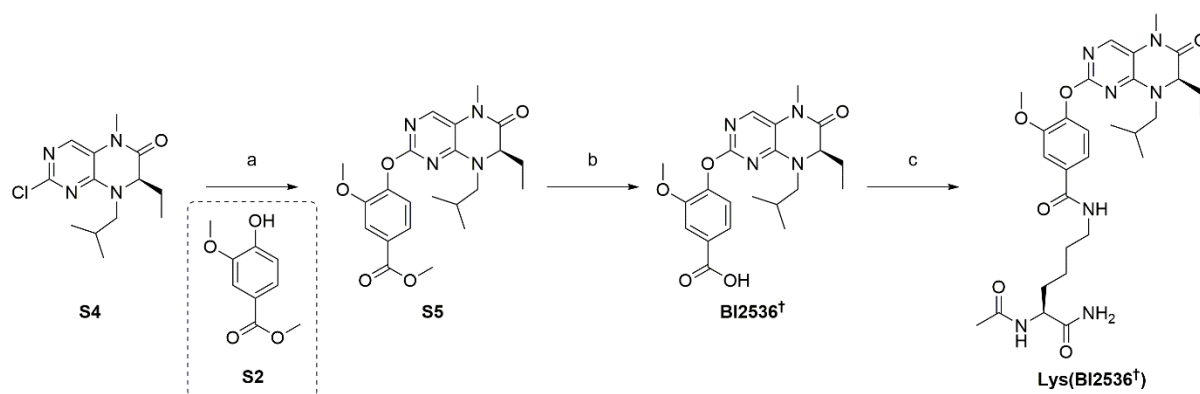
combined with the other flask and stirred at room temperature for 19 h. The mixture was purified by CombiFlash silica gel chromatography (0 to 40% of MeOH in DCM over 25 min) and then using preparative HPLC to afford *N*-((*S*)-5-acetamido-6-amino-6-oxohexyl)-4-(((*R*)-8-cyclopentyl-7-ethyl-5-methyl-6-oxo-5,6,7,8-tetrahydropteridin-2-yl)oxy)-3-methoxybenzamide (**Lys(BI2536\*)**)·2TFA salt (12 mg, 43%) as white to beige powder.

$^1\text{H}$  NMR (400 MHz, MeOD)  $\delta$  7.82 (s, 1H), 7.65 (d,  $J = 2.0$  Hz, 1H), 7.56 (dd,  $J = 8.5$  Hz and 2.0 Hz, 1H), 7.34 (d,  $J = 8.5$  Hz, 1H), 4.43 (dd,  $J = 6.0$  Hz and 3.1 Hz, 1H), 4.31 (dd,  $J = 9.0$  Hz and 5.1 Hz, 1H), 3.86 (s, 3H), 3.69 (quin,  $J = 9.0$  Hz, 1H), 3.42 (t,  $J = 7.0$  Hz, 2H), 3.34 (s, 3H), 2.10 (m, 1H), 1.99 (s, 3H), 1.96–1.77 (m, 4H), 1.74–1.60 (m, 5H), 1.55–1.40 (m, 2H), 1.31–1.17 (m, 2H), 1.16–0.96 (m, 2H), 0.81 (t,  $J = 7.4$  Hz, 3H).

$^{13}\text{C}$  NMR (101 MHz, MeOD)  $\delta$  177.2, 173.4, 168.6, 164.7, 156.8, 154.4, 152.5, 144.6, 135.2, 128.7, 123.6, 121.2, 120.4, 112.9, 65.5, 65.1, 56.6, 54.5, 40.8, 32.8, 30.1, 29.0, 28.8, 28.3, 27.9, 24.8, 24.5, 24.4, 22.5, 8.2.

HRMS (ESI+) calculated for  $\text{C}_{30}\text{H}_{42}\text{N}_7\text{O}_6$ : 596.3191  $[\text{M}+\text{H}]^+$ ; found: 596.3174.

## 6. Synthesis of **Lys(BI2536<sup>†</sup>)**.



**Scheme S4.** Synthesis of **Lys(BI2536<sup>†</sup>)**. (a) **S2**,  $\text{Cs}_2\text{CO}_3$ , DMSO; (b) LiOH, THF/ $\text{H}_2\text{O} = 1:1$ ; (c) Ac-Lys( $\text{NH}_2 \cdot \text{HCl}$ )- $\text{NH}_2$ , HOBt, EDC·HCl, DMF.

(*R*)-2-chloro-7-ethyl-8-isobutyl-5-methyl-7,8-dihydropteridin-6(5H)-one (**S4**, 200 mg, 0.71 mmol)<sup>2</sup> and methyl vanillate (**S2**, 160 mg, 0.85 mmol) were dissolved in DMSO (2.0 mL) and Cs<sub>2</sub>CO<sub>3</sub> (280 mg, 0.85 mmol) was added to the mixture. The reaction mixture was stirred at 90 to 95 °C for 4 d. The mixture was roughly purified by preparative HPLC (0-95% over 30 min) to yield crude methyl (*R*)-4-((8-isobutyl-7-ethyl-5-methyl-6-oxo-5,6,7,8-tetrahydropteridin-2-yl)oxy)-3-methoxybenzoate (**S5**)·2TFA salt (110 mg) as white powder.

**S5** (110 mg, 0.16 mmol) and LiOH (20 mg, 0.81 mmol) were dissolved in a solvent mixture of THF (1.0 mL) and H<sub>2</sub>O (1.0 mL). The reaction mixture was stirred at room temperature for 3 d. The mixture was purified by CombiFlash silica gel column chromatography (0 to 35% of MeOH in DCM over 12 min, and then 35 to 100% of MeOH in DCM over 2 min) to yield (*R*)-4-((7-ethyl-8-isobutyl-5-methyl-6-oxo-5,6,7,8-tetrahydropteridin-2-yl)oxy)-3-methoxybenzoic acid (**BI2536**<sup>†</sup>, 71 mg, 23%, 2steps from **S4**).  
<sup>1</sup>H NMR (400 MHz, MeOD) δ 7.74 (s, 1H), 7.71–7.69 (m, 2H), 7.20 (d, *J* = 8.7 Hz, 1H), 4.18 (dd, *J* = 6.3 Hz and 4.1 Hz, 1H), 3.88 (d, *J* = 10.7 Hz, 1H), 3.78 (s, 3H), 3.58 (dd, *J* = 13.4 Hz and 6.1 Hz, 1H), 3.35 (s, 3H), 2.56 (dd, *J* = 13.5, 8.7 Hz, 1H), 1.92–1.75 (m, 3H), 0.80–0.76 (m, 6H), 0.61 (d, *J* = 6.6 Hz, 3H).

<sup>13</sup>C NMR (101 MHz, MeOD) δ 169.3, 165.3, 161.7, 154.4, 153.1, 147.5, 139.0, 130.1, 123.9, 123.8, 119.1, 114.5, 64.3, 56.3, 53.9, 28.6, 27.3, 26.4, 20.1, 20.1, 9.0.

HRMS (ESI+) calculated for C<sub>21</sub>H<sub>27</sub>N<sub>4</sub>O<sub>5</sub>: 415.1976 [M+H]<sup>+</sup>; found: 415.1963.

To a solution of **BI2536**<sup>†</sup> (24 mg, 0.058 mmol) in DMF (1.5 mL) was added HOBt (8.6 mg, 0.064 mmol) followed by EDC·HCl (11 mg, 0.058 mmol) and stirring at room temperature for 10 min. In the another flask, to a solution of Ac-Lys(NH<sub>2</sub>·HCl)-NH<sub>2</sub> (14 mg, 0.064 mmol) in DMF (1.0 mL) was added DIPEA (22 μL, 0.13 mmol) and the mixture was combined with

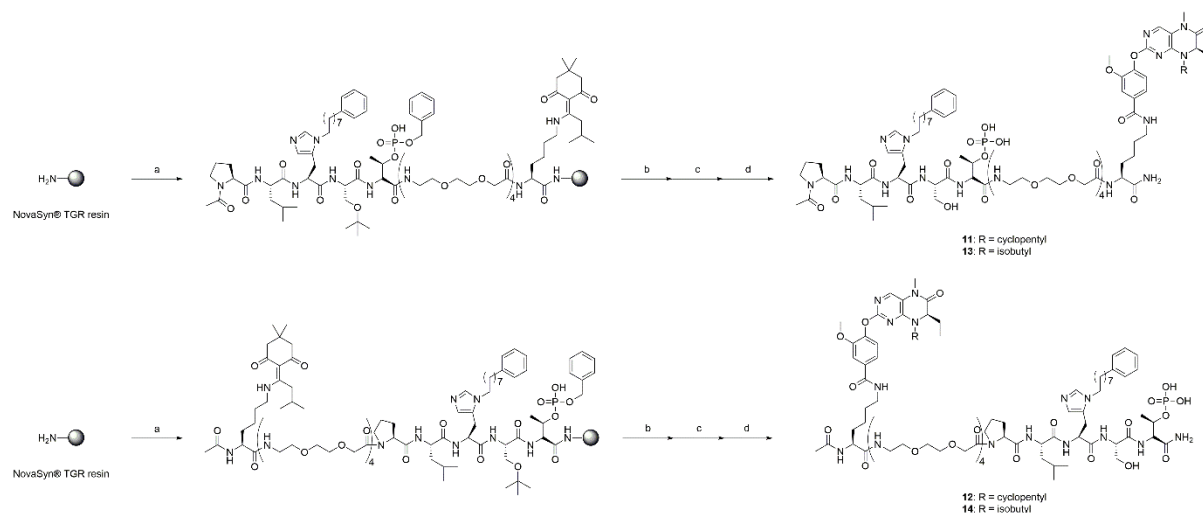
the other flask and stirred at room temperature for 1 d. The mixture was purified by CombiFlash silica gel column chromatography (0 to 40% of MeOH in DCM over 25 min) and then using HPLC to afford *N*-((*S*)-5-acetamido-6-amino-6-oxohexyl)-4-(((*R*)-8-isobutyl-7-ethyl-5-methyl-6-oxo-5,6,7,8-tetrahydropteridin-2-yl)oxy)-3-methoxybenzamide (**Lys(BI2536<sup>+</sup>)**)·2TFA salt (23 mg, 50%).

<sup>1</sup>H NMR (400 MHz, MeOD) δ 7.84 (s, 1H), 7.64 (d, *J* = 1.9 Hz, 1H), 7.55 (dd, *J* = 8.3 Hz and 1.9 Hz, 1H), 7.32 (d, *J* = 8.3 Hz, 1H), 4.36 (dd, *J* = 6.1 Hz and 3.7 Hz, 1H), 4.31 (dd, *J* = 9.0, 5.2 Hz, 1H), 3.84 (s, 3H), 3.54 (dd, *J* = 13.5 Hz and 6.1 Hz, 1H), 3.41 (t, *J* = 7.1 Hz, 2H), 3.35 (s, 3H), 2.75 (dd, *J* = 13.5 Hz and 8.4 Hz, 1H), 2.04–1.79 (m, 7H), 1.75–1.60 (m, 3H), 1.55–1.39 (m, 2H), 0.82–0.78 (m, 6H), 0.59 (d, *J* = 6.6 Hz, 3H).

<sup>13</sup>C NMR (101 MHz, MeOD) δ 177.2, 173.4, 168.8, 164.4, 157.9, 155.0, 152.6, 144.5, 135.0, 129.9, 123.7, 121.0, 119.7, 112.8, 64.3, 56.6, 54.7, 54.5, 40.8, 32.8, 30.1, 28.9, 27.4, 26.7, 24.4, 22.5, 20.1, 20.1, 8.7.

HRMS (ESI<sup>+</sup>) calculated for C<sub>29</sub>H<sub>42</sub>N<sub>7</sub>O<sub>6</sub>: 584.3191 [M+H]<sup>+</sup>; found: 584.3167.

## 7. Synthesis of bivalent ligands 11 – 14.

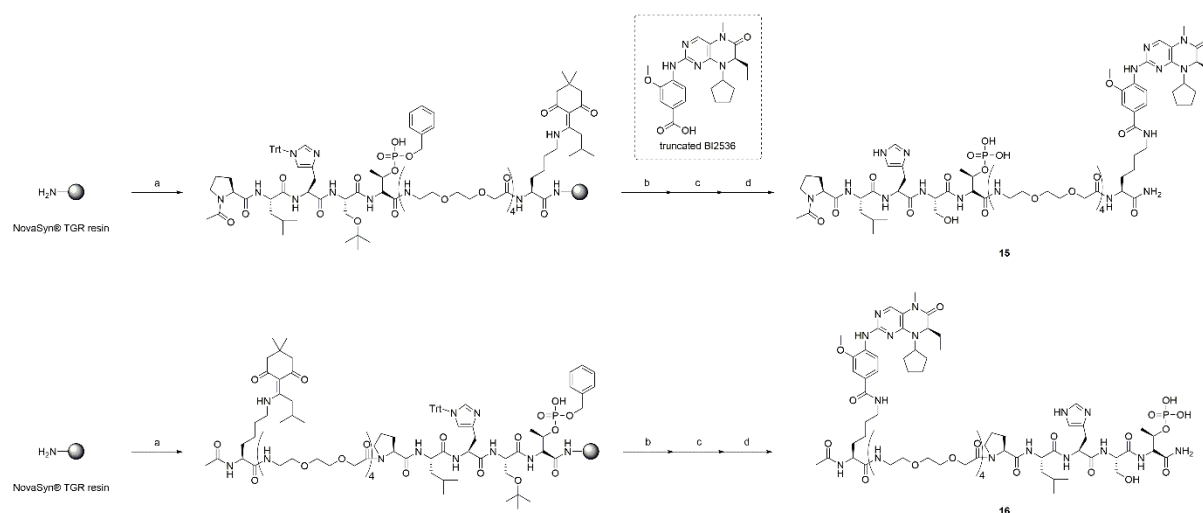


**Scheme S5.** Synthesis of bivalent ligands 11 – 14. (a) Fmoc-based SPPS; (b) 2% (v/v)

hydrazine monohydrate in NMP; (c) **BI2536**\* for **11** and **13** or **BI2536**<sup>†</sup> for **12** and **14**, HATU, DIPEA, NMP; (d) TFA/TIPS/H<sub>2</sub>O = 95:2.5:2.5.

The synthesis of bivalent ligands **11** – **14** was achieved following the general Fmoc-based SPPS protocols mentioned above with the use of **BI2536**\* for **11** and **13** or **BI2536**<sup>†</sup> for **12** and **14** instead of truncated BI2536 for **3** – **10**. The characterized data of these synthesized peptides are shown in the Table S1.

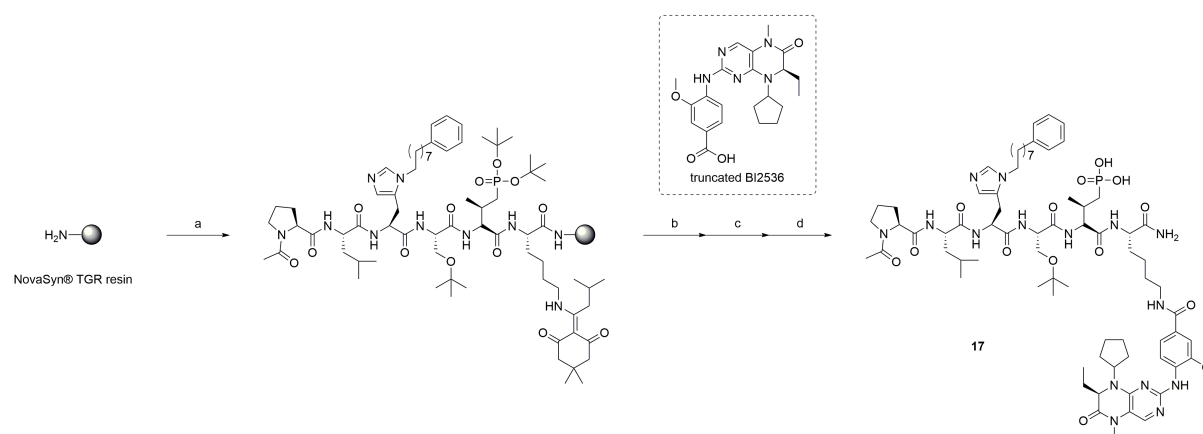
## 8. Synthesis of bivalent ligands 15 and 16.



**Scheme S6.** Synthesis of bivalent ligands **3** – **10**. (a) Fmoc-based SPPS using Fmoc-His(*N*<sup>π</sup>-Trt)-OH instead of Fmoc-His(*N*<sup>π</sup>-(CH<sub>2</sub>)<sub>8</sub>Ph)-OH; (b) 2% (v/v) hydrazine monohydrate in NMP; (c) truncated BI2536, HATU, DIPEA, NMP; (d) TFA/TIPS/H<sub>2</sub>O = 95:2.5:2.5.

The synthesis of bivalent ligands **15** and **16** was achieved following the general Fmoc-based SPPS protocols mentioned above with the use of Fmoc-His(*N*<sup>π</sup>-Trt)-OH instead of Fmoc-His(*N*<sup>π</sup>-(CH<sub>2</sub>)<sub>8</sub>Ph)-OH for **3** – **10**. The characterized data of these synthesized peptides are shown in the Table S1.

## 9. Synthesis of bivalent ligand 17.



**Scheme S7.** Synthesis of bivalent ligands **17**. (a) Fmoc-based SPPS; (b) 2% (v/v) hydrazine monohydrate in NMP; (c) truncated BI2536, HATU, DIPEA, NMP; (d) TFA/TIPS/H<sub>2</sub>O = 95:2.5:2.5.

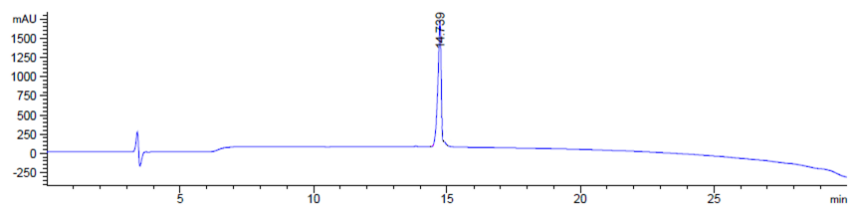
The synthesis of bivalent ligand **17** was achieved following the general Fmoc-based SPPS protocols mentioned above with the use of Fmoc-Pmab(*O**t*-Bu)<sub>2</sub>-OH instead of Fmoc-Thr(PO(OBzl)(OH))-OH for **9**. The characterized data of the synthesized peptide is shown in the Table S1.

**Table S1.** Characterization data of synthesized peptides.

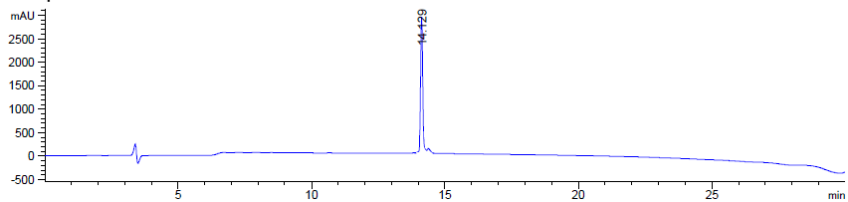
<b>Compound number</b>	<b>Calcd M.W.</b>	<b>Found</b>	<b>Preparative HPLC gradient</b>	<b>Analytical HPLC (10 to 100% of B in A over 30 min) Retention time (<math>t_R</math>, min)</b>
<b>3</b>	660.3 [M + 3H] <sup>3+</sup>	660.5	0 to 80% of B in A over 30 min	14.7
<b>4</b>	660.3 [M + 3H] <sup>3+</sup>	660.5	0 to 80% of B in A over 30 min	14.1
<b>5</b>	917.5 [M + 2H] <sup>2+</sup>	917.5	0 to 60% of B in A over 30 min	14.8
<b>6</b>	917.5 [M + 2H] <sup>2+</sup>	917.5	0 to 70% of B in A over 30 min	14.2
<b>7</b>	772.4 [M + 2H] <sup>2+</sup>	772.5	0 to 70% of B in A over 30 min	15.0
<b>8</b>	772.4 [M + 2H] <sup>2+</sup>	772.5	0 to 70% of B in A over 30 min	14.7
<b>9</b>	699.9 [M + 2H] <sup>2+</sup>	699.8	0 to 75% of B in A over 30 min	15.2
<b>10</b>	1398.7 [M + H] <sup>+</sup>	1398.6	0 to 75% of B in A over 30 min	14.9
<b>11</b>	660.7 [M + 3H] <sup>3+</sup>	660.8	0 to 70% of B in A over 30 min	14.5
<b>12</b>	660.7 [M + 2H] <sup>2+</sup>	660.8	0 to 70% of B in A over 30 min	14.0
<b>13</b>	984.5 [M + 2H] <sup>2+</sup>	984.8	0 to 75% of B in A over 30 min	14.9
<b>14</b>	984.5 [M + 2H] <sup>2+</sup>	984.8	0 to 75% of B in A over 30 min	14.5
<b>15</b>	895.9 [M + 2H] <sup>2+</sup>	896.0	0 to 60% of B in A over 30 min	11.7
<b>16</b>	597.6 [M + 3H] <sup>3+</sup>	597.7	0 to 60% of B in A over 30 min	11.5
<b>17</b>	698.9 [M + 2H] <sup>2+</sup>	698.9	35 to 50% of B in A over 30 min	18.5
<b>FITC-2</b>	678.3 [M + 2H] <sup>2+</sup>	678.3	0 to 70% of B in A over 30 min	16.6

## 10. Analytical HPLC data for peptides 3 – 17 and FITC-2.

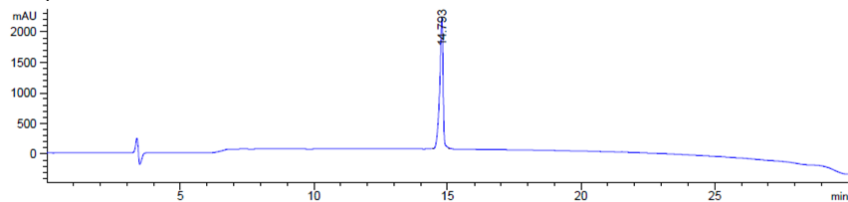
Peptide 3



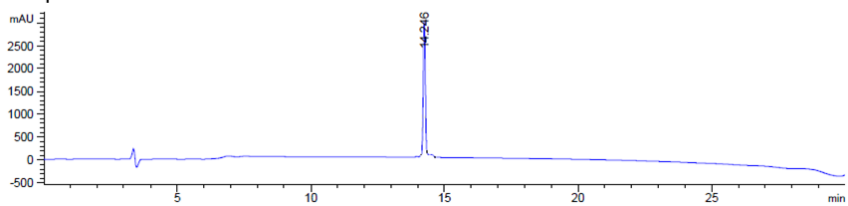
Peptide 4



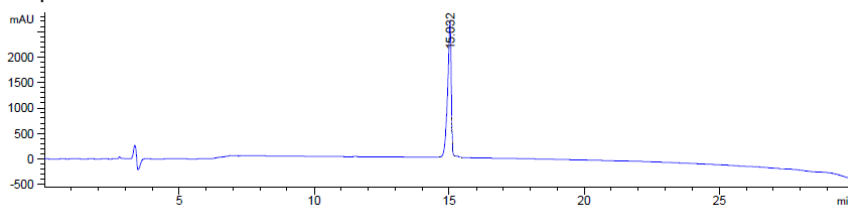
Peptide 5



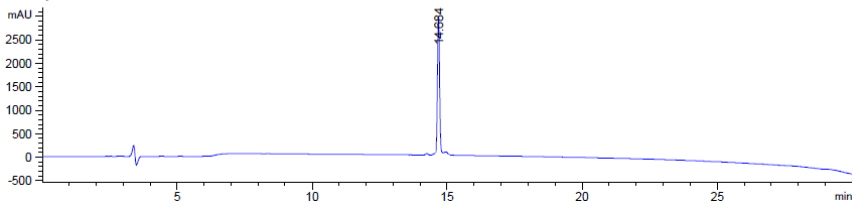
Peptide 6



Peptide 7

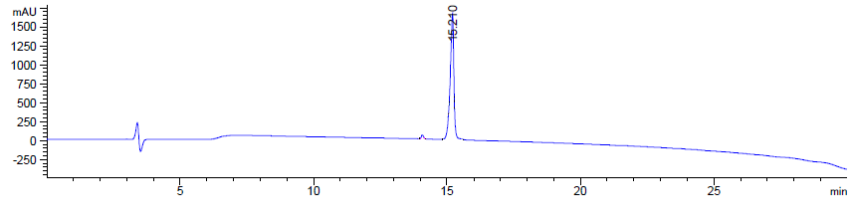


Peptide 8

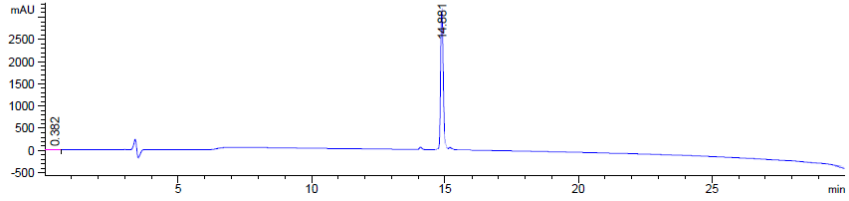




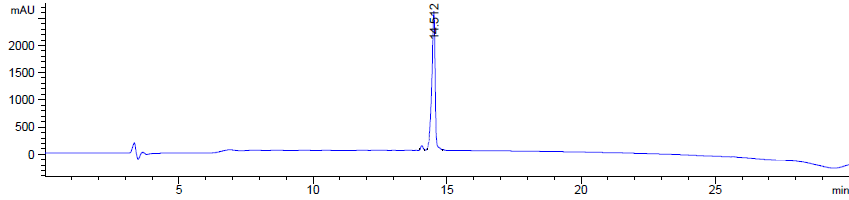
**Peptide 9**



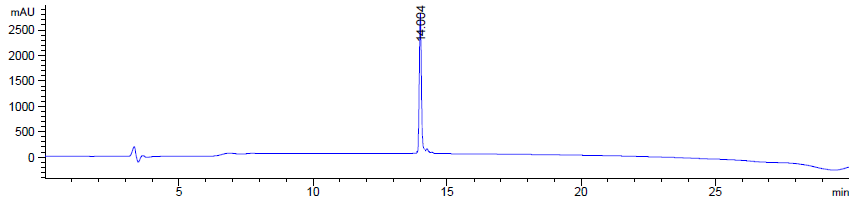
**Peptide 10**



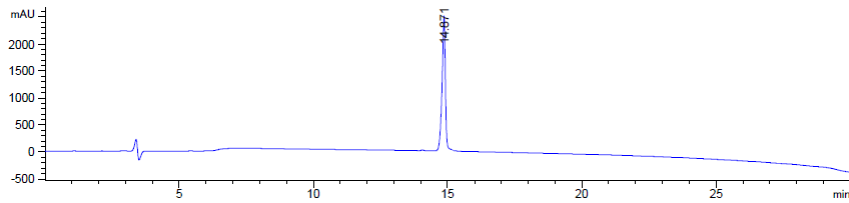
**Peptide 11**



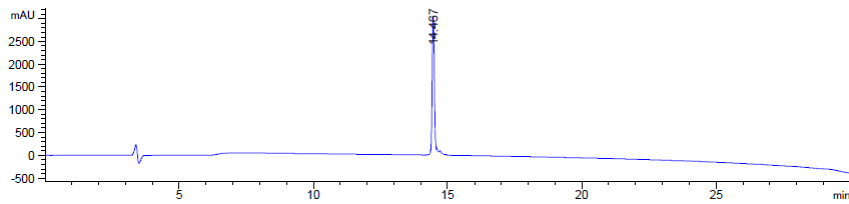
**Peptide 12**



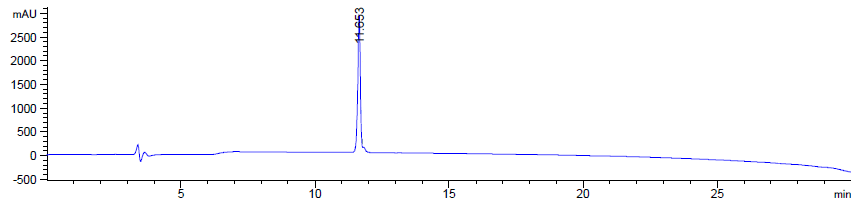
**Peptide 13**



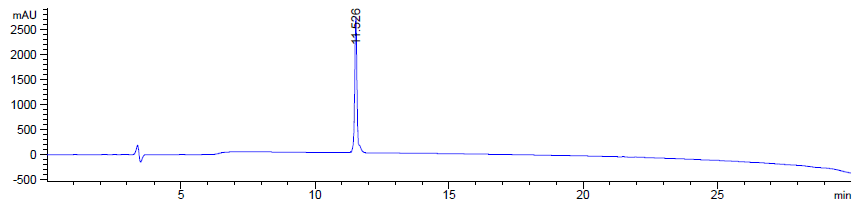
**Peptide 14**



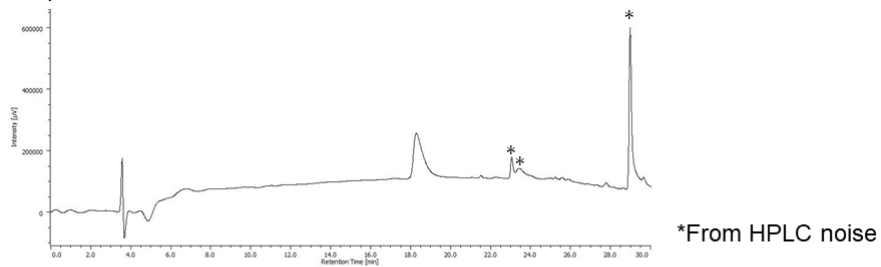
### Peptide 15



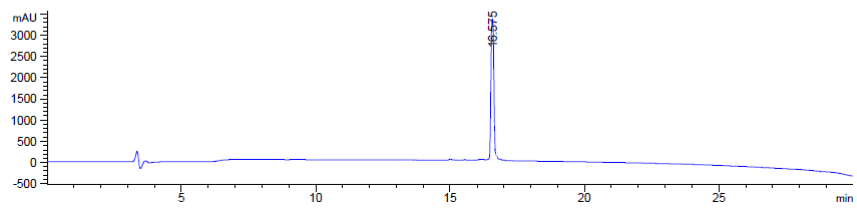
### Peptide 16



### Peptide 17



### FITC-2



## II. BIOLOGICAL EVALUATION

**1. Expression and purification of full-length Polo-like kinase 1 (Plk1) and isolated Plk1 polo-box domain (PBD) for fluorescence polarization (FP) assays, kinase assays, and fluorescence recovery assays.** As previously reported,<sup>3-5</sup> a plasmid encoding myc-tagged full-length Plk1 (Plasmid #41160) and myc-tagged Plk1 PBD (Plasmid #41162) was purchased from Addgene. ~20 M HEK-293T cells (2 x 15 cm plates) were transfected with the plasmid using TurboFect reagent (Thermo Fisher Scientific) according to manufacturer's instructions. Following 48 h expression for full-length Plk1 or 24 h expression for isolated Plk1 PBD, cells were harvested, lysed in buffer [phosphate buffered saline (PBS, pH 7.4) containing 0.5% NP-40 and protease/phosphatase inhibitor (Pierce, Protease and Phosphatase Inhibitor Mini Tablets) cocktail] using freeze/thaw cycles (3x) and centrifuged at 12,500 x G for 10 min at 4 °C. The supernatant containing expressed protein was diluted into 8 mL of PBS (pH 7.4) containing protease/phosphatase inhibitor cocktail. This protein solution was added to a 1 mL bed of myc-agarose resin (Thermo Fisher Scientific) using a disposable 10 mL polypropylene columns (Thermo Fisher Scientific) and allowed to bind for 2 h at 4 °C with gentle rotation. The lysate was removed by filtration and the resin was washed 4x with HBST (HEPES buffered saline (HBS) containing 0.05% Tween-20, 1 mM DTT and 1 mM EDTA) for 10 min with gentle rotation. The bound myc-tagged Plk1 protein was then eluted with a 1 mg/mL solution of myc peptide (EQKLISEEDL) in HBS + 1 mM DTT and 1 mM EDTA. The purified myc-tagged Plk1 was dialyzed 5x with HBS + 1 mM DTT and 1 mM EDTA using a 10 kDa MWCO filter (Sigma, fixed angle rotor at 7,500 x G, 4 °C, 10 min). The concentration of the final protein solution was determined by absorbance at 280 nm and purity was determined by sodium dodecyl sulfate-polyacrylamide gel electrophoresis (SDS-PAGE) with Coomassie staining using NuPAGE™ 4 to 12%, Bis-Tris, 1.0 mm, Mini Protein Gel, 12-well NuPAGE™ Sample Reducing Agent (10X), NuPAGE™ MOPS SDS Running Buffer (20X), SeeBlue™ Plus2 Pre-

stained Protein Standard (Invitrogen), and GelCode™ Blue Safe Protein Stain (Thermo Scientific).

**2. FP assays using purified full-length Plk1 or isolated Plk1 PBD.** Purified protein was diluted to a 2x working dilution in assay buffer (HEPES-buffered saline with 0.05% Tween-20, 1 mM DTT, and 1 mM EDTA) with the final protein concentration representing the approximate  $K_d$  values as determined for the probe **FITC-2**. Inhibitors were serially diluted to generate 4x working dilutions in assay buffer containing 4% DMSO. To each well of a 384-well plate was added 20  $\mu$ L of 2x Plk1 solution (0% binding controls received 20  $\mu$ L of assay buffer). A total of 10  $\mu$ L of the 4x inhibitor solution (or DMSO blank) was added to corresponding wells and allowed to pre-incubate at room temperature for 30 min with shaking. Fluorescent probe **FITC-2** was diluted to 40 nM (4x) in assay buffer and then 10  $\mu$ L was added to each well. The plate was allowed to equilibrate at room temperature for 30 min with shaking. The FP was read using a BioTek Synergy 2 plate reader and PerkinElmer ARVO X5 with 485/20 excitation and 528/20 emission. The FP values were obtained in triplicate and normalized to 100% (no inhibitor) and 0% binding (no protein) controls. Normalized values were plotted versus concentration and analyzed using non-linear regression in GraphPad Prism 8 [log(inhibitor) vs response – variable slope (four parameter) model].  $IC_{50}$  values represent average  $\pm$  standard error of the mean (SEM).

**3. Kinase enzymatic assays using purified full-length Plk1.** The Z'-LYTE™ Kinase Assay Kit - Ser/Thr 16 Peptide (Invitrogen) was used according to manufacturer's instructions using 50 nM Plk1, 20  $\mu$ M ATP, 2  $\mu$ M substrate (or 2  $\mu$ M phosphorylated substrate as 100% control) in the presence of 1% DMSO and 1 mM dithiothreitol (DTT).

**4. Fluorescence recovery assays using purified full-length Plk1.** Fluorescence recovery assay was performed as previously described.<sup>6</sup> Briefly, purified Plk1 was diluted to a 2x working dilution in assay buffer (HEPES-buffered saline with 0.05% Tween-20, 1 mM DTT, and 1 mM EDTA) with the final protein concentration representing the approximate  $K_d$  values as determined for the probe **S6**. Inhibitors were serially diluted to generate 4x working dilutions in assay buffer containing 4% DMSO. To each well of a 384-well plate was added 20  $\mu$ L of 2x Plk1 solution (0% binding controls received 20  $\mu$ L of assay buffer). A total of 10  $\mu$ L of the 4x inhibitor solution (or DMSO blank) was added to corresponding wells and allowed to pre-incubate at room temperature for 30 min with shaking. Fluorescent probe **S6** were diluted to 80 nM (4x) in assay buffer and then 10  $\mu$ L was added to each well. The plate was allowed to equilibrate at room temperature for 30 min with shaking. The fluorescence intensity was read using a BioTek Synergy 2 plate reader and PerkinElmer ARVO X5 with 485/20 excitation and 528/20 emission. The fluorescence intensity values were obtained in triplicate and normalized to 100% (no inhibitor) and 0% binding (no protein) controls. Normalized values were plotted versus concentration and analyzed using non-linear regression in GraphPad Prism 8 [log(inhibitor) vs response – variable slope (four parameter) model].  $IC_{50}$  values represent average  $\pm$  standard error of the mean (SEM).

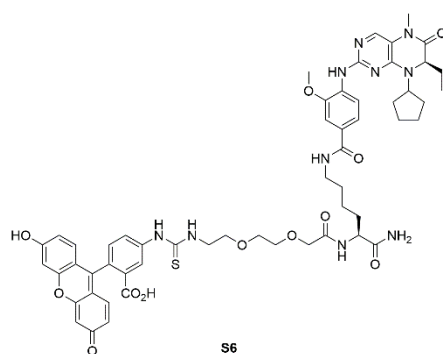


**Figure S1.** The structure of probe **S6**.

**5. MTT assays using HeLa cells.** MTT assays were performed as following procedure: HeLa cells (JCRB9004, the Japanese Collection of Research Bioresources (JCRB) Cell Bank, Osaka, Japan) were seeded in a 96-well plate ( $5 \times 10^3$  cells/well) with 100  $\mu$ L of Dulbecco's modified Eagle's medium (D-MEM) supplemented with 10% fetal bovine serum (FBS), 2 mM L-Gln, 100  $\mu$ g/ml of penicillin, and 100  $\mu$ g/ml of streptomycin for each wells. After 1 day incubation at 37 °C, the media were replaced with the serially diluted compounds containing media, and cells were incubated at 37 °C for additional 2 days. The cells were washed with PBS (200  $\mu$ L x1) and the generated formazan was dissolved in 200  $\mu$ L of 4 M HCl aq./2-propanol (0.1:10). The absorbance of each wells at 565 nm were read using iMark Microplate Reader (BIO-RAD). The absorbance values were obtained in triplicate and normalized to 100% (no inhibitor) and 0% viability (no cell) controls. Normalized values were plotted versus concentration and analyzed using non-linear regression in GraphPad Prism 9 [log(inhibitor) vs response – variable slope (four parameter) model]. IC<sub>50</sub> values represent average  $\pm$  standard error of the mean (SEM).

**6. Immunostaining experiments using HeLa cells.** HeLa cells were seeded in a 35 mm glass-bottom dish (12 mm radius glass area, AGC TECHNO GLASS CO., LTD., Shizuoka, Japan) at a density of  $1 \times 10^4$  cells/dish 200  $\mu$ L of D-MEM supplemented with 10% FBS, 2 mM L-Gln, 100  $\mu$ g/ml of penicillin, and 100  $\mu$ g/ml of streptomycin. After 1 day incubation at 37 °C, the media were replaced with the media with or without each concentrations of compounds (BI2536: 15 nM and **17**: 10  $\mu$ M), and the cells were incubated at 37 °C for additional 1 days. The cells were washed with PBS (200  $\mu$ L x2) and fixed with 4% paraformaldehyde phosphate buffer solution (FUJIFIRM Wako Pure Chemical Corporation, Japan) for 15 min at room temperature, and then washed with PBS (200  $\mu$ L x2). The fixed cells were treated with 0.1% Triton X-100 (FUJIFIRM Wako Pure Chemical Corporation) in PBS

(200  $\mu$ L) for 10 min at room temperature and washed with PBS (200  $\mu$ L x2), and then blocked with 1% bovine serum albumin (BSA, Sigma-Aldrich) in PBS for 30 min at room temperature. The cells were incubated with 200  $\mu$ L of primary antibody solution (Plk1 Monoclonal Antibody (35-206, Mouse IgG1 kappa), Cat#: 37-7000 invitrogen/alpha Tubulin Polyclonal Antibody (Rabbit IgG), Cat#: PA5-81281, invitrogen/1% BSA in PBS = 2:1:100) at 4  $^{\circ}$ C overnight. The cells were washed with PBS (200  $\mu$ L x3) for 10 min each, and then treated with 200  $\mu$ L of secondary antibody solution (Goat Anti-Mouse IgG H&L (Alexa Fluor<sup>®</sup> 647), Cat#: ab150115, abcam/Goat anti-Rabbit IgG (H+L) Cross-Adsorbed Secondary Antibody, Alexa Fluor<sup>™</sup> 488, Cat#: A-11008, Invitrogen/PBS = 1:1:1000) at room temperature for 30 min. The cells were washed with PBS (200  $\mu$ L x3) for 10 min each. Subsequently, nucleic acids were stained with 200  $\mu$ L of 4',6-diamidino-2-phenylindole (DAPI) solution (1 mg/mL buffer, DOJINDO, Japan) in PBS (1:1000) at room temperature for 10 min. The cells were washed with PBS (200  $\mu$ L x2) and added 200  $\mu$ L of PBS. Confocal laser scanning microscopic (CLSM) observations were performed using a FluoView FV10i (Olympus, Tokyo, Japan).

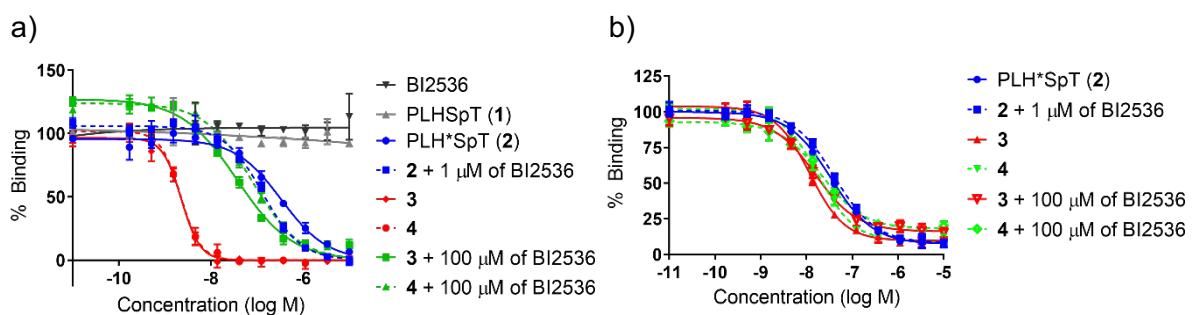


**Figure S2.** Results from fluorescence polarization (FP) assays, which measured the ability of Plk1 inhibitors to compete with FITC-2 for binding to (a) full-length Plk1 or (b) isolated Plk1 PBD. The X axis represents inhibitor concentration (log M) and the Y axis represents relative probe binding based on the FP (Ex: 485 nm, Em: 528 nm) of no inhibitor (100%) and blank

(no protein, 0%). Data points represent average  $\pm$  SEM from three independent experiments and fit using non-linear regression in GraphPad Prism 8.

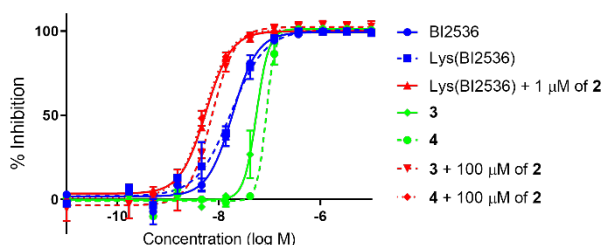


**Figure S3.** Results from kinase assays, which measured the inhibitory potencies of the test compounds in a catalytic assay using full-length Plk1 (Z'-LYTE™ kinase assay kit - Ser/Thr 16 Peptide, Invitrogen). The X axis represents inhibitor concentration (log M) and the Y axis represents % inhibition based on the % phosphorylation of the substrate. The calculation was conducted according to the manufacturer's instructions. Data points represent average  $\pm$  SEM from three independent experiments and fit using non-linear regression in GraphPad Prism 8.

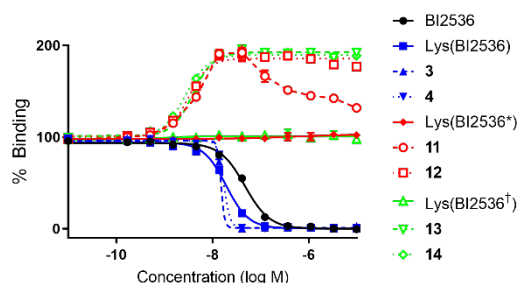


**Figure S4.** Results from fluorescence recovery assays, which measured the ability of Plk1 inhibitors to compete with S6 for binding to full-length Plk1. The X axis represents inhibitor concentration (log M) and the Y axis represents relative probe binding based on the fluorescence intensity (Ex: 485 nm, Em: 528 nm) of no inhibitor (100%) and blank (no protein, 0%). Data points represent average  $\pm$  SEM from three independent experiments and fit using non-linear regression in GraphPad Prism 8.



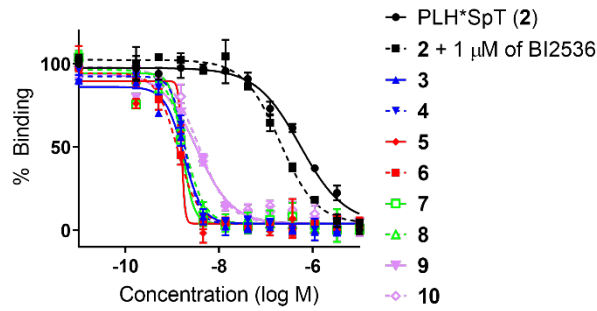


**Figure S5.** Results from fluorescence polarization (FP) assays, which measured the ability of Plk1 inhibitors to compete with FITC-2 for binding to full-length Plk1. The X axis represents inhibitor concentration (log M) and the Y axis represents relative probe binding based on the FP (Ex: 485 nm, Em: 528 nm) of no inhibitor (100%) and blank (no protein, 0%). Data points represent average  $\pm$  SEM from three independent experiments and fit using non-linear regression in GraphPad Prism 8.

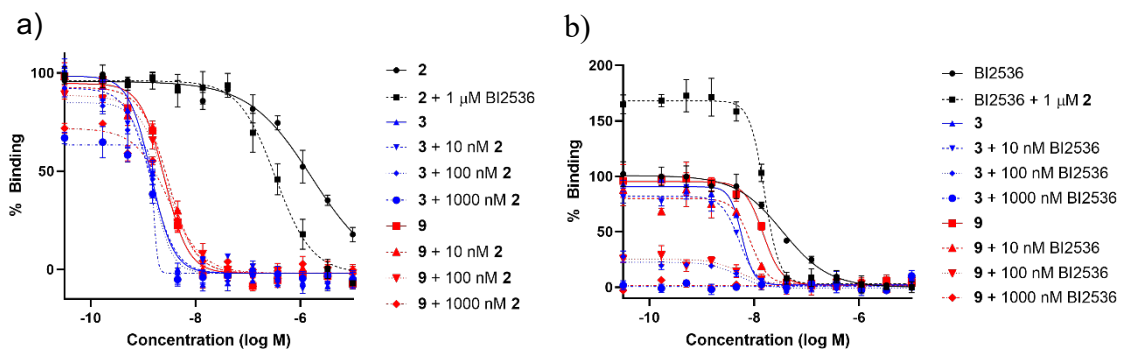


**Figure S6.** Results from (a) fluorescence polarization (FP) assays, which measured the ability of Plk1 inhibitors to compete with FITC-2 for binding to full-length Plk1 and from fluorescence recovery assays, which measured the ability of Plk1 inhibitors to compete with S6 for binding to full-length Plk1. The X axis represents inhibitor concentration (log M), and the Y axis represents relative probe (FITC-2) binding based on the FP (Ex: 485 nm, Em: 528 nm) of no inhibitor (100%) and blank (no protein, 0%) or relative probe (S6) binding based on the fluorescence intensity (Ex: 485 nm, Em: 528 nm) of no inhibitor (100%) and blank (no

protein, 0%). Data points represent average  $\pm$  SEM from three independent experiments and fit using non-linear regression in GraphPad Prism 9.

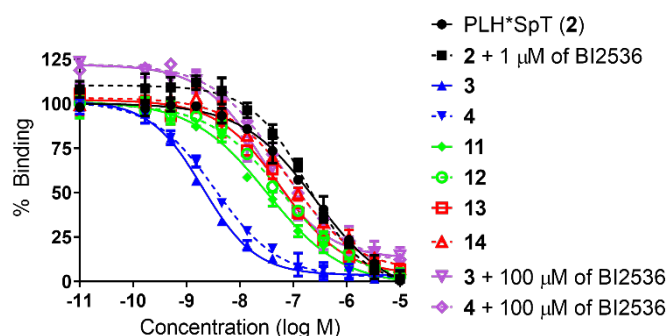


**Figure S7.** Results from fluorescence polarization (FP) assays, which measured the ability of Plk1 inhibitors to compete with FITC-2 for binding to full-length Plk1. The X axis represents inhibitor concentration (log M) and the Y axis represents relative probe binding based on the FP (Ex: 485 nm, Em: 528 nm) of no inhibitor (100%) and blank (no protein, 0%). Data points represent average  $\pm$  SEM from three independent experiments and fit using non-linear regression in GraphPad Prism 8.

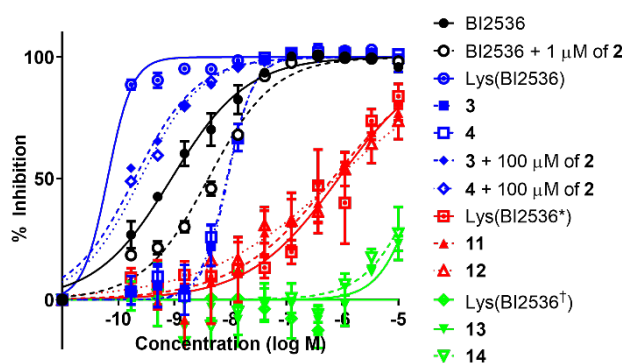


**Figure S8.** Results from kinase assays, which measured the inhibitory potencies of the test compounds in a catalytic assay using full-length Plk1 (Z'-LYTE™ kinase assay kit - Ser/Thr 16 Peptide, Invitrogen). The X axis represents inhibitor concentration (log M) and the Y axis represents % inhibition based on the % phosphorylation of the substrate. The calculation was conducted according to the manufacturer's instructions. Data points represent average  $\pm$  SEM from three independent experiments and fit using non-linear regression in GraphPad Prism 8.

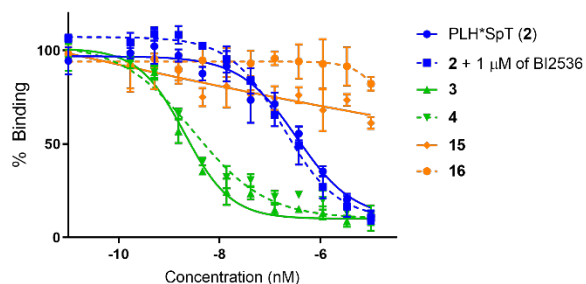


**Figure S9.** Results from fluorescence polarization (FP) assays, which measured the ability of Plk1 inhibitors to compete with FITC-2 for binding to full-length Plk1. The X axis represents inhibitor concentration (log M) and the Y axis represents relative probe binding based on the FP (Ex: 485 nm, Em: 528 nm) of no inhibitor (100%) and blank (no protein, 0%). Data points represent average  $\pm$  SEM from three independent experiments and fit using non-linear regression in GraphPad Prism 8.

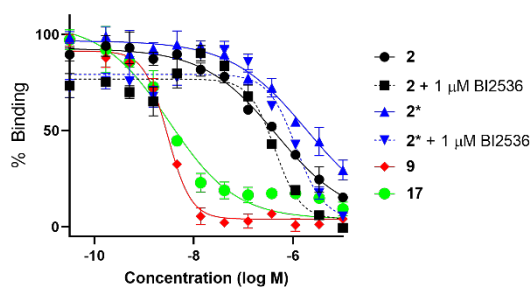


**Figure S10.** Results from fluorescence polarization (FP) assays, which measured the ability of Plk1 inhibitors to compete with FITC-2 for binding to full-length Plk1. The X axis represents inhibitor concentration (log M) and the Y axis represents relative probe binding based on the FP (Ex: 485 nm, Em: 528 nm) of no inhibitor (100%) and blank (no protein, 0%). Data points represent average  $\pm$  SEM from three independent experiments and fit using non-linear regression in GraphPad Prism 9.

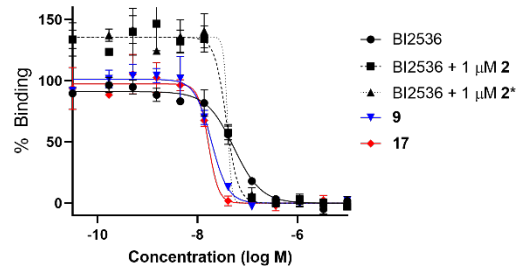


**Figure S11.** Results from fluorescence recovery assays, which measured the ability of Plk1 inhibitors to compete with S6 for binding to full-length Plk1. The X axis represents inhibitor concentration (log M) and the Y axis represents relative probe binding based on the fluorescence intensity (Ex: 485 nm, Em: 528 nm) of no inhibitor (100%) and blank (no protein, 0%). Data points represent average  $\pm$  SEM from three independent experiments and fit using non-linear regression in GraphPad Prism 9.

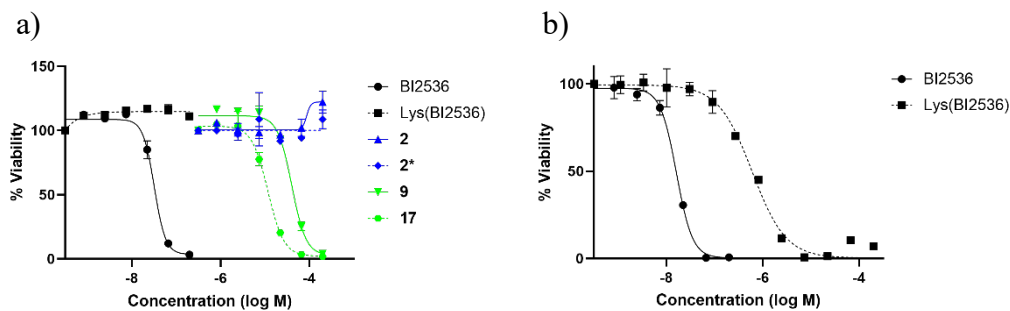


**Figure S12.** Results from MTT assays, which measured the viability of HeLa cells with treatment of the Plk1 inhibitors. The X axis represents inhibitor concentration (log M) and the Y axis represents relative cell viability based on the absorbance intensity at 565 nm of no inhibitor (100%) and blank (no cells, 0%). Data points represent average  $\pm$  SEM from three independent experiments and fit using non-linear regression in GraphPad Prism 9.

### III. MOLECULAR DYNAMICS SIMULATIONS

Two approaches were used to construct full-length plk1 structure. First, we examined the stability of Plk1 with the KD and PBD as in the structure of isolated zebrafish polo-kinase 1 KD and PBD with *drosophila* MAP205 peptide (PDB code 4J7B). Using the 4J7B structure as a template, an homology model was built using the Swiss-model webserve.<sup>7</sup> The ligands of BI2536 and PLHSpT (peptide **1**) were mapped into the homology model by superimposing the crystal structures of KD –bound BI2536 (PDB 2RKU) and PBD – bound PLH\*SpT (**2**), where H\* indicates the presence of a  $-(\text{CH}_2)_8\text{Ph}$  group on the His N3( $\pi$ ) nitrogen [ie, H\* = His-[N( $\pi$ )-( $\text{CH}_2$ )<sub>8</sub>Ph] (PDB 3RQ7), respectively. In the second approach, the KD and PBD domain conformation obtained from the first approach were docked together using the protein docking program megadock.<sup>8</sup> Employing a megadock pose as the reference, the PDB structures 2RKU and 3RQ7 were superimposed onto the KD and PBD domain, and then manually adjusted to allow better protein – protein interaction and simultaneous binding of ligands **9** and **10**. The linker conformations were randomly selected in the second approach.

The systems were solvated by TIP3P water molecules, and sodium and chloride ions were added to neutralize the system and to achieve a total concentration of ~150 mM (Table S2). The systems were energy minimized for 50000 conjugate gradient steps. In the equilibration stage, each system was gradually relaxed by a series of dynamic cycles. In the production stage, all simulations were performed using the NPT ensemble at 310 K. All molecular dynamics (MD) simulations were performed using the NAMD software<sup>9</sup> with CHARMM36 force field.<sup>10</sup> The short-range van der Waals interactions were calculated using the switching function, with a twin range cut-off of 10.0 Å and 12.0 Å. The long-range electrostatic interactions were calculated with the Particle Mesh Ewald method with a cut-off of 12.0 Å. MD trajectories were saved by every 2 ps for analysis.

**Table S2.** Molecular dynamics simulation parameters.

<b>Simulation System</b>	<b>Box Size (<math>\text{\AA}^3</math>)</b>	<b>Total Number of Atoms</b>
Apo	$120 \times 117 \times 129$	94049
BI2536	$89 \times 101 \times 108$	92520
PLHSpT (1)	$89 \times 101 \times 108$	92464
BI2536 + 1	$99 \times 125 \times 132$	111762
<b>9</b>	$98 \times 84 \times 93$	72364
<b>10</b>	$98 \times 86 \times 93$	73410

#### IV. CELL MEMBRANE PERMEABILITY ANALYSIS

The Caco-2 cell permeability assays were performed by Charles River Laboratories (Worcester, MA, USA) with their own confidential procedure. Ranitidine, Talinolol\_NI (no inhibitor), Talinolol\_VERA (in the presence of 25  $\mu\text{M}$  of verapamil), and Warfarin were used as low permeability control, P-gp efflux control, P-gp efflux control with P-gp inhibitor, and high permeability control, respectively. The results of the assays were summarized in Table S3.

**Table S3.** Results from the Caco-2 cell permeability assays.

Compound	Assay concentration ( $\mu\text{M}$ )	Mean $P_{\text{app}}$ A-B ( $10^{-6}$ cm/s)	Mean $P_{\text{app}}$ B-A ( $10^{-6}$ cm/s)	Mean (B-A/A-B) Efflux Ratio	Mean A-B % Recovery	Mean B-A % Recovery	A-B Permeability Ranking
BI2536	10	4.76	11.5	2.41	58.2%	71.6%	Higher
<b>2</b>	10	0.0660	0.0283	0.428	69.4%	72.1%	Lower
<b>2*</b>	10	0.0148	0.0197	1.33	81.8%	75.0%	Lower
<b>17</b>	10	0.001440	0.0129	8.94	65.2%	67.1%	Lower
Ranitidine	10	0.227	0.527	2.33	91.3%	86.0%	Lower
Talinolol_NI	10	0.344	3.88	11.3	91.4%	91.3%	Lower
Talinolol_VERA	10	0.708	1.18	1.67	90.1%	88.8%	Lower
Warfarin	10	39.4	21.4	0.542	91.2%	84.0%	Higher

Study#: RT-0008-DV-PB. Incubation time: 2 hours. Permeability Ranking: lower is  $< 1 \times 10^{-6}$  cm/s; higher is  $> 1 \times 10^{-6}$  cm/s. An efflux ratio  $> 2$  indicates potential for the compound to be a substrate for P-gp or other active transporter.

## REFERENCES

1. Budin, G.; Yang, K. S.; Reiner, T.; Weissleder, R., Bioorthogonal probes for polo-like kinase 1 imaging and quantification. *Angew. Chem. Int. Ed. Eng.* **2011**, *50* (40), 9378-9381.
2. Chen, L.; Yap, J. L.; Yoshioka, M.; Lanning, M. E.; Fountain, R. N.; Raje, M.; Scheenstra, J. A.; Strovel, J. W.; Fletcher, S., BRD4 structure–activity relationships of dual PLK1 kinase/BRD4 bromodomain inhibitor BI-2536. *ACS Med. Chem. Lett.* **2015**, *6* (7), 764-769.
3. Zhao, X. Z.; Hymel, D.; Burke, T. R., Jr., Application of oxime-diversification to optimize ligand interactions within a cryptic pocket of the polo-like kinase 1 polo-box domain. *Bioorg. Med. Chem. Lett.* **2016**, *26* (20), 5009-5012.
4. Zhao, X. Z.; Hymel, D.; Burke, T. R., Jr., Enhancing polo-like kinase 1 selectivity of polo-box domain-binding peptides. *Bioorg. Med. Chem.* **2017**, *25* (19), 5041-5049.
5. Hymel, D.; Burke, T. R., Jr., Phosphatase-stable phosphoamino acid mimetics that enhance binding affinities with the polo-box domain of polo-like kinase 1. *ChemMedChem* **2017**, *12* (3), 202-206.
6. Tsuji, K.; Hymel, D.; Burke, T. R., Jr., A new genre of fluorescence recovery assay to evaluate polo-like kinase 1 ATP-competitive inhibitors. *Anal. Methods* **2020**, *12* (36), 4418-4421.
7. Waterhouse, A.; Bertoni, M.; Bienert, S.; Studer, G.; Tauriello, G.; Gumienny, R.; Heer, F. T.; de Beer, T. A P.; Rempfer, C.; Bordoli, L.; Lepore, R.; Schwede, T., SWISS-MODEL: homology modelling of protein structures and complexes. *Nucleic. Acids Res.* **2018**, *46* (W1), W296-W303.
8. Ohue, M.; Shimoda, T.; Suzuki, S.; Matsuzaki, Y.; Ishida, T.; Akiyama, Y., MEGADOCK 4.0: an ultra-high-performance protein–protein docking software for heterogeneous supercomputers. *Bioinformatics* **2014**, *30* (22), 3281-3283.



9. Kalé, L.; Skeel, R.; Bhandarkar, M.; Brunner, R.; Gursoy, A.; Krawetz, N.; Phillips, J.; Shinozaki, A.; Varadarajan, K.; Schulten, K., NAMD2: Greater scalability for parallel molecular dynamics. *J. Comput. Phys.* **1999**, *151* (1), 283-312.
10. MacKerell, A. D.; Bashford, D.; Bellott, M.; Dunbrack, R. L.; Evanseck, J. D.; Field, M. J.; Fischer, S.; Gao, J.; Guo, H.; Ha, S.; Joseph-McCarthy, D.; Kuchnir, L.; Kuczera, K.; Lau, F. T. K.; Mattos, C.; Michnick, S.; Ngo, T.; Nguyen, D. T.; Prodhom, B.; Reiher, W. E.; Roux, B.; Schlenkrich, M.; Smith, J. C.; Stote, R.; Straub, J.; Watanabe, M.; Wiórkiewicz-Kuczera, J.; Yin, D.; Karplus, M., All-atom empirical potential for molecular modeling and dynamics studies of proteins. *J. Phys. Chem. B* **1998**, *102* (18), 3586-3616.